Quasi-integrable systems based on the symplectic integrators (SI).

PERSONNEL

- *Principal Investigator:* Stanislav Baturin, Northern Illinois University, Assistant Professor. Theory, experiment design, data analysis, preliminary simulations.
- Alexander Romanov, Fermilab, Scientist. Machine operation, lattice design, data acquisition, data processing.

PURPOSE AND METHODS

A. Motivation

The concept of integrable and quasi-integrable nonlinear optics has recently attracted significant attention. Initially suggested by Danilov (see Ref.[1] and references therein) and refined by Danilov and Nagaitsev in Ref.[2], the concept has been expanded to more realistic cases with space charge and chromaticity effects accounted for [3, 4]. Experimental demonstration of the integrable optics concept is currently being conducted at the IOTA facility at Fermilab [5, 6] as well as at UMER ring at the University of Maryland [7].

The main idea behind the integrable optics concept is a special insert of nonlinear magnets that is accommodated by a purely linear ring. The system is arranged in a way that the effective Hamiltonian for the lattice is almost time-independent and the potential produced by one nonlinear magnet warrants separation of variables, and thus a second integral of motion [2, 8]. Initial designs of the nonlinear insert considered for the initial experiments at IOTA [6] were based on an idea of approximating the smooth nonlinear potential with a certain number of nonlinear magnets (17 in the case of IOTA octupole inset and nonlinear magnet insert) with their strength scaled according to a prescription derived in Ref.[2] and placed equidistantly. Questions remain whether this number could be reduced further, and if the performance and design of the nonlinear insert could be further enhanced.

In Ref.[9] this question was addressed and a new method of designing a nonlinear lattice based on known symplectic integration methods was proposed.

It was shown that octupole nonlinear insert at IOTA could be implemented with just five magnets. A new arrangement was suggested as well as new relative scaling law. It was predicted as well that it is possible to implement quasi-integrable optics with just thee nonlinear magnets (Yoshida lattice) that are strategically placed along the ring.

In this proposal we suggest to probe both ideas (modification of the octupole channel and Yoshida lattice) experimentally.

B. Theoretical background

It is known that integral of motion in the case of purely linear system (parabolic potential) is a Hamiltonian in normalized coordinates. Below we expand on this idea and try to preserve some smooth Hamiltonian in normalized coordinates with the nonlinear potential by designing proper lattice.

The connection between a smooth Hamiltonian system and a map (lattice usually could be reduced to some mapping) naturally arises from building an integrator that is essentially a discrete analog of a smooth system by definition [10, 11]. The more accurate the integrator, the better it reproduces dynamics of the original system. In this section we give a brief derivation of the specific forms of the known integrators that we are going to utilize further.

We consider a smooth Hamiltonian of the form

$$\mathrm{H} = \sum_{i=1}^{2} \frac{q_i^2 + p_i^2}{2} + V(q_1, q_2). \tag{1}$$

Here V is the nonlinear potential of the form

$$V(q_1, q_2) = \sum_{j=3}^{l} a_j P_j(q_1, q_2), \tag{2}$$

We split the Hamiltonian into a part that corresponds to linear motion

$$\mathrm{H}_1 = \sum_{i=1}^{2} \frac{q_i^2 + p_i^2}{2} \tag{3}$$

and a part

$$\mathrm{H}_2 = V(q_1, q_2) \tag{4}$$

that combines all nonlinearities. Now if we consider a time mesh, $t = mh$ $m \in \mathbb{N}$, with a step h, then the one step integrator Ψ_h of the Hamiltonian H will have the from

$$\Psi_h = R_h \circ K_h. \tag{5}$$

This is a well known symplectic Euler method. Here R_h is a matrix of rotations that corresponds to the flow of the hamiltonian (3) and K_h is a thin nonlinear kick (a flow of the Hamiltonian (4)) given by

$$K_h X_0 = [q_1^0, p_1^0 - h\partial_{q_1} V, q_2^0, p_2^0 - h\partial_{q_2} V]^{\mathrm{T}}, \tag{6}$$

with each partial derivative taken at the initial point (q_1^0, q_2^0). Here X_0 is the vector of initial conditions $X_0 = [q_1^0, p_1^0, q_2^0, p_2^0]^{\mathrm{T}}$. It is known that Euler method (5) conserves the Hamiltonian $H = H_1 + H_2$ up to the order $\mathscr{O}(h)$ and consequently is accurate only for quite small steps in phase.

To preserve Hamiltonian with higher accuracy on the same mesh several high order integration methods were developed in the late 1990 beginning of 2000 (see for example Ref.[11]). The first method that has accuracy of $\mathscr{O}(h^2)$ in preservation of Hamiltonian (1) was introduced to accelerator community by Ruth Ref.[12]:

$$\Phi_h = R_{h/2} \circ K_h \circ R_{h/2}. \tag{7}$$

Integrator that preserves the Hamiltonian up to the order $\mathscr{O}(h^4)$ is the three step Yoshida integrator [13–15].

$$\Phi_h^Y = \Phi_{\gamma_3 h} \circ \Phi_{\gamma_2 h} \circ \Phi_{\gamma_1 h}. \tag{8}$$

with corresponding gammas given by

$$\gamma_1 = \gamma_3 = \frac{1}{2 - 2^{1/3}}, \quad \gamma_2 = -\frac{2^{1/3}}{2 - 2^{1/3}}. \tag{9}$$

Following Ref.[9] to avoid negative time steps we use the identity $R_{2\pi} = \mathscr{I}$ and write the integrator (8) in the final form as

$$\begin{aligned}\Phi_h^Y =& R_{\gamma_1 h/2} \circ K_{\gamma_1 h} \circ R_{2\pi-\kappa_1 h/2} \\ & \circ K_{-\kappa_2 h} \circ R_{2\pi-\kappa_1 h/2} \circ K_{\gamma_1 h} \circ R_{\gamma_1 h/2}, \\ \gamma_1 =& \frac{1}{2-2^{1/3}},\ \kappa_1 = \frac{2^{1/3}-1}{2-2^{1/3}},\ \kappa_2 = \frac{2^{1/3}}{2-2^{1/3}}.\end{aligned} \tag{10}$$

To establish a connection between integrators in normalized coordinates $\{q_1, p_1, q_2, p_2\}$ and a real optical lattice, we recall that propagation of the particle from position s_1 to position s_2 through a linear optical channel could be described using a block diagonal transfer matrix [16] with the block of the type

$$\begin{aligned}&M_{x,y}(s_2|s_1) = \\ &\mathbf{B}_{x,y}(s_2) \begin{bmatrix} \cos(\psi_{x,y}) & \sin(\psi_{x,y}) \\ -\sin(\psi_{x,y}) & \cos(\psi_{x,y}) \end{bmatrix} \mathbf{B}_{x,y}^{-1}(s_1).\end{aligned} \tag{11}$$

Here, the lower index denotes coordinate pair (either $\{x, P_x\}$ or $\{y, P_y\}$); $\psi_{x,y} = \int_{s_1}^{s_2} \frac{ds}{\beta_{x,y}(s)}$ is the phase advance between position s_1 and s_2; $\mathbf{B}_{x,y}(s)$ is the corresponding block of the betatron amplitude matrix and $\mathbf{B}_{x,y}^{-1}(s)$ its inverse given by [16]

$$\begin{aligned}\mathbf{B}_{x,y}(s) &= \begin{bmatrix} \sqrt{\beta_{x,y}(s)} & 0 \\ -\frac{\alpha_{x,y}(s)}{\sqrt{\beta_{x,y}(s)}} & \frac{1}{\sqrt{\beta_{x,y}(s)}} \end{bmatrix}, \\ \mathbf{B}_{x,y}^{-1}(s) &= \begin{bmatrix} \frac{1}{\sqrt{\beta_{x,y}(s)}} & 0 \\ \frac{\alpha_{x,y}(s)}{\sqrt{\beta_{x,y}(s)}} & \sqrt{\beta_{x,y}(s)} \end{bmatrix}.\end{aligned} \tag{12}$$

Here $\beta_{x,y}(s)$, and $\alpha_{x,y}(s) = -1/2\beta'_{x,y}(s)$ are the Twiss parameters of the linear lattice.

Now let us consider an integrator, Ψ_h, given by (7) and propagate a vector of initial conditions for one step, h, that corresponds to the phase advance between points, s_2 and s_1, of a linear lattice

$$X_h = R_{h/2} \circ K_h \circ R_{h/2} X_0. \tag{13}$$

With the identity $\mathscr{I} = \mathbf{B}(s) \circ \mathbf{B}^{-1}(s)$ (here $\mathscr{I}$ is the identity matrix) equation (13) transforms as

$$\mathrm{X}_h = M(s_2|s_1) \circ \mathbf{B}(s_1) \circ K_h \circ \mathbf{B}^{-1}(s_1) \circ M(s_1|s_0) \mathrm{X}_0. \tag{14}$$

Here, X denotes the unnormalized state vector $\mathrm{X}_{h,0} \equiv \mathbf{B} X_{h,0}$.

We evaluate $\mathbf{B}(s_1) \circ K_h \circ \mathbf{B}^{-1}(s_1)$ further to achieve nonlinear element strength scaling with the β-function in a form

$$N^\beta \mathrm{X}_0 = \left[x^0, P_x^0 - h\frac{\partial_x U}{\sqrt{\beta_x}}, y^0, P_y^0 - h\frac{\partial_y U}{\sqrt{\beta_y}} \right], \tag{15}$$

with

$$\partial_{x,y} U = \partial_{q_1,q_1} V(q_1, q_2)\ q_1 \to \frac{x}{\sqrt{\beta_x}}, q_2 \to \frac{y}{\sqrt{\beta_y}}. \tag{16}$$

The two building blocks of the integrator are the flows R_h and K_h, that now with the help of the Eq.(11), Eq.(15) and Eq.(16) could be transformed to $M(s_2|s_1)$ and N^β respectively. Maps $M(s_2|s_1)$ and N^β could be implemented with thin lenses in a real lattice.

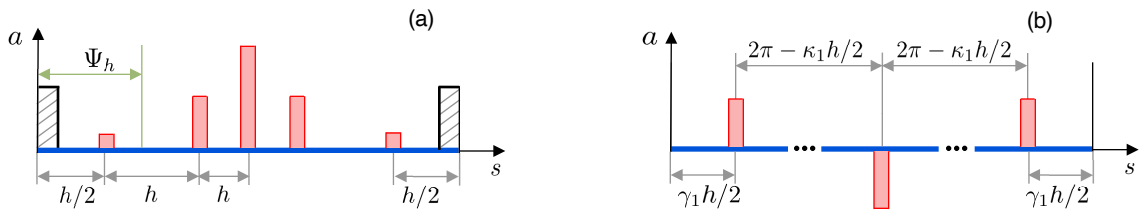

FIG. 1. Schematic diagrams of the nonlinear magnet layout for one period of the lattice: (a) Ruth lattice, based on Ruth second order integrator (7) and Yoshida lattice (c) based on Yoshida integrator (10). Here s is the longitudinal spatial coordinate and a is the normalized magnitude of the nonlinear magnets, h is the phase advance between the magnets, multipliers γ_1 and κ_1 for Yoshida lattice are given by Eq(10).

C. Experimental setup

1. *Octupole channel*

A schematic layout of the proposed experiment is shown in Fig.1(a). All machine parameters should be the same as for the initial experiments with the nonlinear insert. Machine lattice is arrange as a T-insert as prescribed in Ref.[2] - a linear focusing matrix in both x and y directions. β - functions in the drift where oclupoles are placed should be equal.

As it follows from Eq.(15) and Eq.(16) scaling of the octupoles with respect to the β - function should be

$$a_{\Psi}^{(4)} \sim \frac{1}{\beta^2(s_i)}. \tag{17}$$

Here, s_i - is the physical position of the i-th thin octupole in the lattice. Octupoles have to be place according to the condition of the constant phase advance. Positions s of the octupoles are calculated on a constant phase mesh by numerically inverting formula for the phase advance in the drift

$$\psi(s) = \arctan\left(\sqrt{\frac{kL}{4-kL}}\right) - \arctan\left(\frac{\sqrt{k}L - 2\sqrt{k}s}{\sqrt{L(4-kL)}}\right). \tag{18}$$

Several sets of distances between the magnets that correspond to a given machine tune are listed in the Table I corresponding diagrams of octupole channel operation are shown in Fig.2.

TABLE I. Physical positions inside the drift in meters for the octupole magnets. Zero ($s = 0$) is taken at the point $\beta_x = \beta_y$. Position in s is taken at the magnet center. Full length of the octupole channel is 1.8 m.

ν_f	h	s_1	s_2	s_3	s_4	s_5
0.148	0.188	0.2	0.562	0.9	1.238	1.6
0.237	0.297	0.238	0.6	0.9	1.2	1.562
0.366	0.46	0.37	0.7	0.9	1.1	1.43

For the head to head comparison it is suggested to collect data for the lattice of 5 octupoles with original scaling

$$a_{\mathrm{DN}}^{(4)} \sim \frac{1}{\beta^3(s_i)}. \tag{19}$$

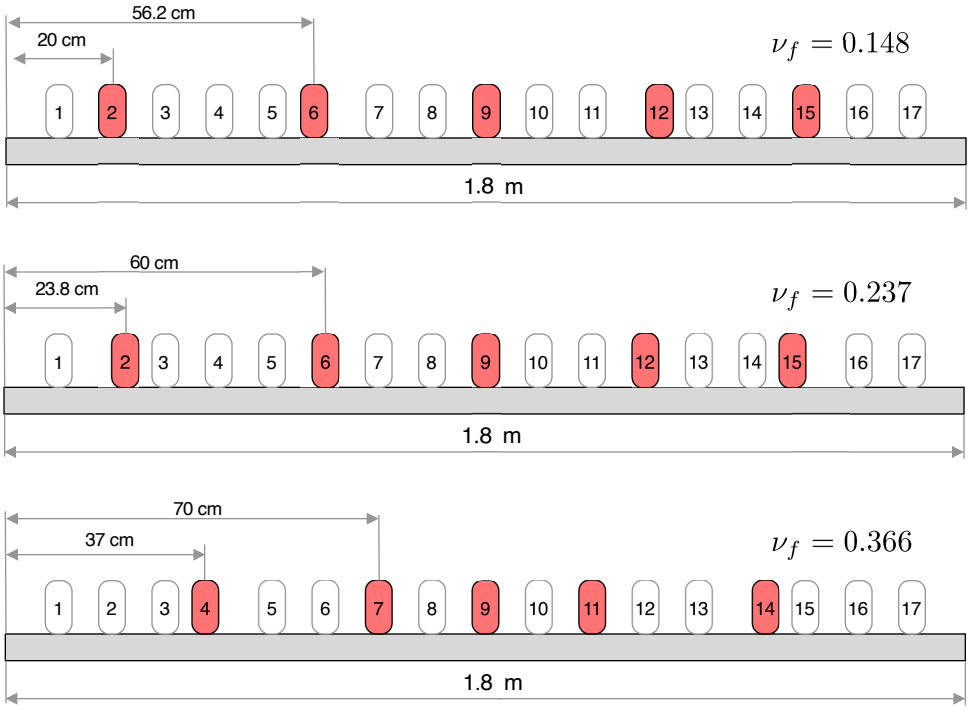

FIG. 2. Schematic diagrams of the octupole channel operation for the Ruth lattice. Red color indicates magnets that are turned on, white is for the magnets that are completely turned off. Equidistant phase placement and scaling with the β-function as given by Eq.(17) in Ref.[9].

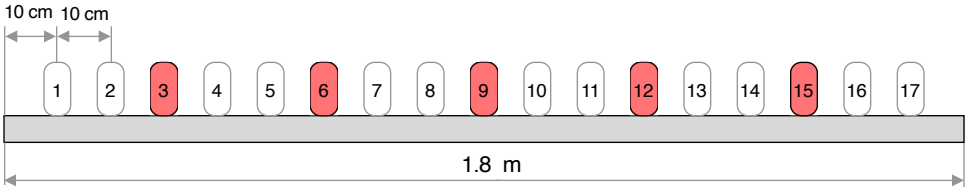

FIG. 3. Schematic diagrams of the octupole channel operation for the base line measurements. Red color indicates magnets that are turned on, white is for the magnets that are completely turned off. Equidistant magnet placement and scaling with the β-function as given by Eq.(19) in Ref.[2].

and equal distances between the magnets (0.3 m), the way it is currently designed (by simply turning down 12 of 17 octupoles). On pattern for the octuples for this comparison is 3,6,9,12,15 as shown on figure Fig.3.

First the data (turn by turn BPM data and SyncLight data [17]) is collected for the unmodified octupole channel. Then for the same machine tune octupoles are physically moved to satisfy condition of the equal phase advance and experiment is repeated.

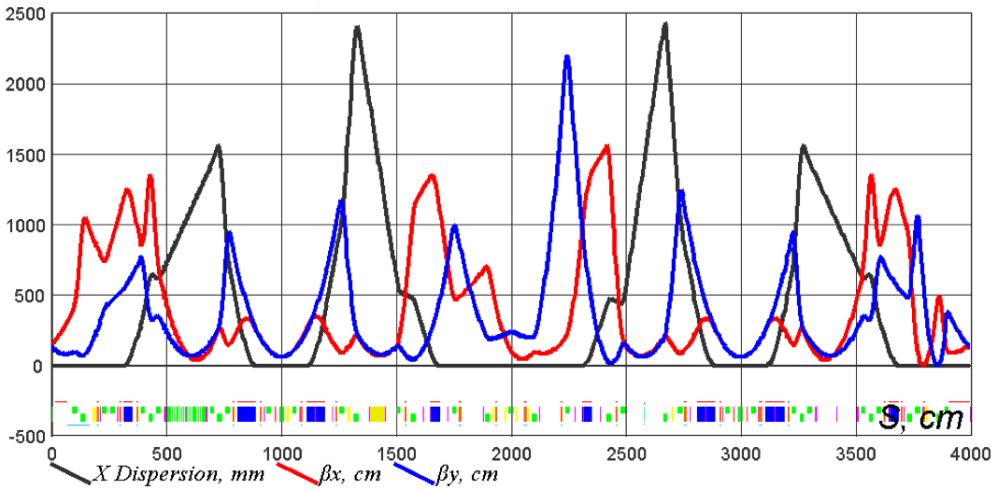

FIG. 4. Yoshida lattice for the IOTA ring. Approximate sextupole positions are 970 cm, 1027 cm and 3025 cm.

2. *Yoshida lattice*

Schematics of the Yoshida lattice is shown in Fig.1(b). According to the integrator formula Eq.(10) three nonlinear magnets have to be separated by three drifts that are calculated according the step h and coefficients γ_1,γ_2, γ_3. It should be noted that phase advance between first and second and second and third magnets is large.

For the proof of principle experiment it is suggested to use three of four IOTA sextupoles that are located symmetrically in pair on the opposite sides of the ring. According to the Eq.(15) and Eq.(16) scaling of the sextupoles with respect to the β - function should be

$$a_{\Psi}^{(3)} \sim \frac{1}{\beta^{3/2}(s_i)}. \tag{20}$$

Here, as before s_i - is the physical position of the i-th sextupole in the lattice. Additional scaling comes from corresponding gammas as well. It is worth noting that second magnet have to have inverted polarity with respect to other two.

TABLE II. Yoshida lattice parameters for different fractional tunes of the ring.

ν_f	h	$\gamma_1 h/2$	$2\pi - \kappa_1 h/2$
0.05	0.3142	$0.0338\times 2\pi$	$0.9912\times 2\pi$
0.1	0.6283	$0.0676\times 2\pi$	$0.9824\times 2\pi$
0.15	0.9425	$0.1013\times 2\pi$	$0.9737\times 2\pi$

Conditions on the phase advance between sextupoles are listed in the Table II for different values of fractional tune ν_f. Parameter h is connected to the fractional tune ν_f though the relation

$$\nu_f = \frac{h}{2\pi}. \tag{21}$$

The following additional conditions on the linear optics should be met:

1) Phase advance between the sextupoles in x is equal to Phase advance in y.

2) β-functions are equal at the positions of the sextupoles.

3) Dispersion is zero at the positions of the sextupoles.

4) Tune of the ring have to be chosen such that $h < 1$.

An example of IOTA lattice that fulfill conditions above is shown in the Fig.4.

D. Expected results and sources of uncertainty

We expect to demonstrate that suggested lattice indeed close reproduce dynamics of the smooth Henon-Heiles system. We are going to extract transverse phase space from the BPM data and build Poincare surface of sections for the Ruth lattice with octupoles Fig.5(a) and for the Yoshida lattice with sextupoles Fig.5. We expect to observe characteristic beam shape on the SyncLight system (quasi rectangular for the octupoles and triangular for the sextupoles) as well as to detect tuneshifts due to the nonliearities and try to cross certain resonances (1/3, 1/4, 1/2). As additional indirect evidence we plan to demonstrate conservation of corresponding Henon-Heiles Hamiltonian in normalized coordinates.

Main source of uncertainty is the phase advance between the nonlinear magnets as well as mismatch in the machine tune. From the preliminary simulations we see that 5% variation in both is acceptable and will still allow us to reach the goal.

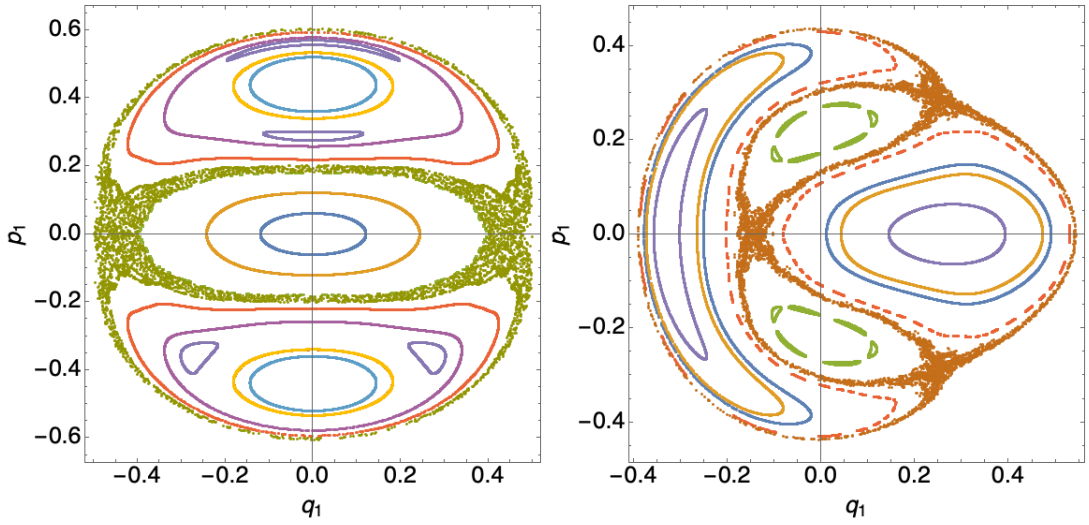

FIG. 5. Simulated poincare surface of sections for the Ruth octupole lattice (left) and for the Yoshida sextupole lattice (right).

BEAM CONDITIONS

- **Species:** electron
- **Energy:** any energy between 70 - 150 MeV
- **Intensity:** Main operating mode is regular beam injection. Intensity could be any known intensity that could be successfully detected by the BPMs and SyncLight.

- **Number of bunches, transverse emittance, beam size, bunch length, momentum spread:** No specific requirements to the beam parameters.
- **Injection time structure:** Inject the beam to the central orbit. Kick the beam, record BPM and SyncLight signals. Reinjection on beam loss, no specific timing.
- **Orbit:** central orbit for the injection and calibrations.
- **Lattice parameters:** Octupole experiment requires the same lattice as any experiment with the nonlinear channel. Equal β functions in the drift and the ring set as T-insert. For the Yoshida lattice, required optics is shown in Fig.4.

APPARATUS

No specific apparatus is needed except what is already installed and commissioned at the IOTA ring is needed. For the octupole experiment access to the basic bench work tools is desirable.

RUN PLAN

E. Experiment with Octupoles (Ruth lattice)

- Record turn-by-turn data for beam kicked in X and/or Y planes for a range of kick amplitudes and octupoles settings in original configuration with reduced number of powered octupoles: 1-2 half-shift (4h each, frequent injections)
  - may be a part of original octupoles studies
- IOTA hall access to relocate octupoles: 4h
- Record turn-by-turn data for beam kicked in X and/or Y planes for a range of kick amplitudes and octupoles settings: 2-3 half-shifts (4h each, frequent injections)
- IOTA hall access to return octupoles to original positions: 4h

F. Experiment with Sextupoles (Yoshida lattice)

- Tune injection lattice of FAST to match beam with SNL lattice: 4h
- Inject beam and tune IOTA lattice: 2 half-shifts and 1 full shift: 2x4h and 8h
- Record turn-by-turn data for beam kicked in X and/or Y planes for a range of kick amplitudes and sextupoles settings: 2-3 half-shifts (4h each, frequent injections)

[1] V. Danilov, "Practical solutions for nonlinear accelerator lattice with stable nearly regular motion," *Phys. Rev. ST Accel. Beams*, vol. 11, p. 114001, Nov 2008.

[2] V. Danilov and S. Nagaitsev, "Nonlinear accelerator lattices with one and two analytic invariants," *Phys. Rev. ST Accel. Beams*, vol. 13, p. 084002, Aug 2010.

[3] S. Webb, D. Bruhwiler, A. Valishev, S. Nagaitsev, and V. Danilov, "Chromatic and Space Charge Effects in Nonlinear Integrable Optics," in *Proceedings of the ICFA Advanced Beam Dynamics Workshop on High-Intensity and High-Brightness Hadron Beams (54th ICFA, HB2014), November 10-14, 2014*, p. 216, JACoW, East-Lansing, MI, 2014.

[4] S. Nagaitsev and A. Valishev, "Beam Physics of Integrable Optics Test Accelerator at Fermilab," in *Proceedings of the 3rd International Particle Accelerator Conference (IPAC'12), New Orleans, LA, May 20-25, 2012*, p. 1371, IEEE, Piscataway, NJ, 2012.

[5] S. Antipov, D. Broemmelsiek, D. Bruhwiler, D. Edstrom, E. Harms, V. Lebedev, J. Leibfritz, S. Nagaitsev, C. Park, H. Piekarz, P. Piot, E. Prebys, A. Romanov, J. Ruan, T. Sen, G. Stancari, C. Thangaraj, R. Thurman-Keup, A. Valishev, and V. Shiltsev, "IOTA (integrable optics test accelerator): facility and experimental beam physics program," *Journal of Instrumentation*, vol. 12, pp. T03002–T03002, mar 2017.

[6] S. Antipov, S. Nagaitsev, and A. Valishev, "Single-particle dynamics in a nonlinear accelerator lattice: attaining a large tune spread with octupoles in IOTA," *Journal of Instrumentation*, vol. 12, pp. P04008–P04008, apr 2017.

[7] K. Ruisard, H. B. Komkov, B. Beaudoin, I. Haber, D. Matthew, and T. Koeth, "Single-invariant nonlinear optics for a small electron recirculator," *Phys. Rev. Accel. Beams*, vol. 22, p. 041601, Apr 2019.

[8] C. Mitchell, "Complex representation of potentials and fields for the nonlinear magnetic insert of the Integrable Optics Test Accelerator," *arXiv:1908.00036*, 2019.

[9] S. S. Baturin, "Hamiltonian preserving nonlinear optics," *arXiv:1908.03520*, 2019.

[10] M. Tabor, *Chaos and integrability in nonlinear dynamics : an introduction*. New York : Wiley, 1989.

[11] E. Hairer, C. Lubich, and G. Wanner, *Geometric numerical integration : structure-preserving algorithms for ordinary differential equations*. Bernil; New York: Springer, 2006.

[12] R. D. Ruth, "A canonical integration technique," *IEEE Transactions on Nuclear Science*, vol. 30, pp. 2669–2671, Aug 1983.

[13] E. Forest, "Canonical integrators as tracking codes (or how to integrate perturbation theory with tracking)," *AIP Conference Proceedings*, vol. 184, no. 1, pp. 1106–1136, 1989.

[14] M. Suzuki, "Fractal decomposition of exponential operators with applications to many-body theories and monte carlo simulations," *Physics Letters A*, vol. 146, no. 6, pp. 319 – 323, 1990.

[15] H. Yoshida, "Construction of higher order symplectic integrators," *Physics Letters A*, vol. 150, no. 5, pp. 262 – 268, 1990.

[16] S. Y. Lee, *Accelerator Physics*. World Scientific Publishing, 2012.

[17] N. Kuklev, Y. Kim, and A. Romanov, "Synchrotron Radiation Beam Diagnostics for the Integrable Optics Test Accelerator," in *Proc. 9th International Particle Accelerator Conference (IPAC'18), Vancouver, BC, Canada, April 29-May 4, 2018*, no. 9 in International Particle Accelerator Conference, (Geneva, Switzerland), pp. 2073–2076, JACoW Publishing, June 2018.